

# Fracture behaviour of liquid crystal epoxy resin systems based on the diglycidyl ether of 4,4'-dihydroxy- $\alpha$ -methylstilbene and sulphanilamide

## Part I *Effects of curing variations*

H. J. SUE

*Polymer Technology Center, Department of Mechanical Engineering, Texas A&M University, College Station, TX 77843-3123 USA*

J. D. EARLS, R. E. HEFNER, Jr

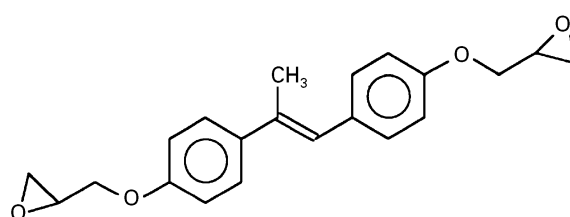
*Organic Product Research, B-1215, The Dow Chemical Company, Freeport, TX 77541 USA*

The fracture behaviours of the pour-cast, unoriented diglycidyl ether of 4,4'-dihydroxy- $\alpha$ -methylstilbene/sulphanilamide liquid crystalline epoxies (LCE) cured at various temperature steps are investigated. It is found that, depending on how the LCE is cured, the liquid crystalline (LC) domain size varies dramatically. These, in turn, affect how the LCEs fracture. The operative toughening mechanisms in the toughest LCE are studied in detail and found to include the formation of numerous segmented, unlinked microcracks in front of the main crack. When the crack opens up, the matrix material between the segmented microcracks acts as a bridge between the opening crack planes. Furthermore, crack bifurcation appears to take place when the segmented cracks are eventually linked with the main crack. This entire fracture process accounts for the high fracture toughness ( $G_{IC} = 580 \text{ J m}^{-2}$ ) of this particular LCE with respect to conventional epoxies ( $G_{IC} = 180 \text{ J m}^{-2}$ ). The relationship between the LCE morphology and the corresponding fracture mechanisms is discussed.

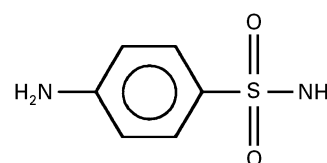
### 1. Introduction

Recent research and development of the diglycidyl ether of 4,4'-dihydroxy- $\alpha$ -methylstilbene (DGE-DHAMS) based liquid crystalline epoxy (LCE) resin systems has shown that these LCEs possess excellent chemical, physical, mechanical, and rheological characteristics suitable for high performance automotive, electronic and aerospace structural applications [1–5]. That is, these LCEs can exhibit extremely high tensile modulus and strength when molecularly oriented, high fracture toughness, high ductility, outstanding chemical and solvent resistance, high  $T_g$ , low water absorption, and ease of processing. The LC domain size and type (either in amorphous, in nematic, or in smectic form) and molecular orientation can be controlled via combination(s) of cure temperature, curing agent, and external fields (mechanical shearing, electrical and magnetic field alignments) during curing [6–8]. With all the advantages denoted above, LCEs have a strong potential to become the next generation epoxies for high performance coatings, electronics, and structural applications.

The chemical structures of the DGE-DHAMS and sulphanilamide curing agent to be used in this study are given below:



DGE-DHAMS



Sulphanilamide

When the DGE-DHAMS monomers slowly cool from a melting temperature of  $130^\circ\text{C}$  to temperatures between  $95$  and  $56^\circ\text{C}$ , nematic LC domains will form [1]. At temperatures higher than  $95^\circ\text{C}$ , these nematic LC domains are not present; only the isotropic state is observed. Nevertheless, when the monomer molecular

weight begins to build upon curing, even at temperatures higher than 95 °C, the LC domains will evolve and maintain the LC characteristics [1, 8].

The directionality and degree of orientation of the LC phase for the LCE and curable blends thereof can be controlled and enhanced by the application of either mechanical, electrical or magnetic fields. Since the state of orientation of LC domains can greatly affect the physical and mechanical properties of LCEs, the control of the directionality and degree of orientation of LC domains are important aspects of evaluating LCEs for structural applications. This area of research is, however, subject to our future investigations. The fracture behaviour of the unoriented LCEs will be studied first and is the subject of this paper.

Until now, effort on the investigation of the fracture behaviour of LCEs has been scarce. Knowledge concerning the link between the LC morphology and the corresponding fracture process is even less emphasized. The present work, as part of a larger effort in gaining fundamental understanding and improving molecular/morphological designs of LCEs, attempts to study the fracture behaviour of the unoriented DGE-DHAMS/sulphanilamide system using both fracture mechanics and microscopy tools. The effects of curing variations in the LC domain morphology and the corresponding fracture process are investigated. It is hoped that the source of toughening in the DGE-DHAMS/sulphanilamide system can be identified and the relationships between the LC domain, morphology, and fracture mechanisms in LCEs can be understood and established.

## 2. Experimental procedure

The synthesis, chemical structures, and physical and rheological properties of the LCEs based on DGE-DHAMS/sulphanilamide system have been reported elsewhere [1, 4, 6]. Only the experiments relevant to the present study will be described below.

In curing the DGE-DHAMS/sulphanilamide LCEs, three different conditions were adopted in this study:

1. 4 h @120 °C + 1 h @140 °C + 1 h @160 °C + 1 h @180 °C + 6 h @200 °C (LCE-1)
2. 4 h @160 °C + 1 h @180 °C + 6 h @200 °C (LCE-2)
3. 4 h @200 °C (LCE-3)

LCE-1 was cured in such a way that sufficient time was given, by gradually raising the curing temperatures, for the LC monomers to form LC domains before extensive cross-linking took place. LCE-3, on the other hand, was cured in such a way that it cross-linked rapidly and minimum time was allowed for the LCE monomers to align and form LC domains. LCE-2 was cured in an intermediate fashion. These three curing conditions were expected to produce very different LC morphologies in the matrix.

After the LCE resins were cured and slowly cooled to room temperature (25 °C) in the oven, the 0.635 cm-thick LCE plaques were machined into bars with

dimensions of 6.35 × 1.27 × 0.635 cm for the single-edge-notch three-point-bend (SEN-3PB) fracture toughness measurements and with dimensions of 12.7 × 1.27 × 0.635 cm for the double-notch four-point-bend (DN-4PB) experiments (Fig. 1) [9–11]. These bars were then notched with a notch-cutter (250 μm tip radius), followed by liquid nitrogen-chilled razor blade tapping to wedge open a sharp crack. The ratio between the final crack length and the specimen width was held between 0.3 and 0.7 [12, 13].

A Sintech-2 screw-driven mechanical testing machine was used to conduct a tensile test at 0.508 cm/min., SEN-3PB and the DN-4PB experiments, at a cross-head speed of 0.508 mm min<sup>-1</sup>. For the 3PB-F test, a cross-head speed of 0.125 cm min<sup>-1</sup> was adopted. The tensile modulus was determined based on the ASTM D638 method. The SEN-3PB method was utilized for fracture toughness measurement, i.e. plane strain critical stress intensity factor ( $K_{IC}$ ), following the procedures described in the literature [13]. The critical strain energy release rate ( $G_{IC}$ ) is calculated based on

$$G_{IC} = \frac{K_{IC}^2(1 - \nu^2)}{E}$$

where  $E$  is Young's modulus and  $\nu$  is Poisson's ratio. When the DN-4PB experiment was performed, care was taken to ensure that the upper contact loading points were touching the specimen simultaneously.

For transmitted optical microscopy (TOM) investigations, thin sections ( $\approx 40 \mu\text{m}$ ) of the mid-section (plane strain region) of the DN-4PB crack tip damage

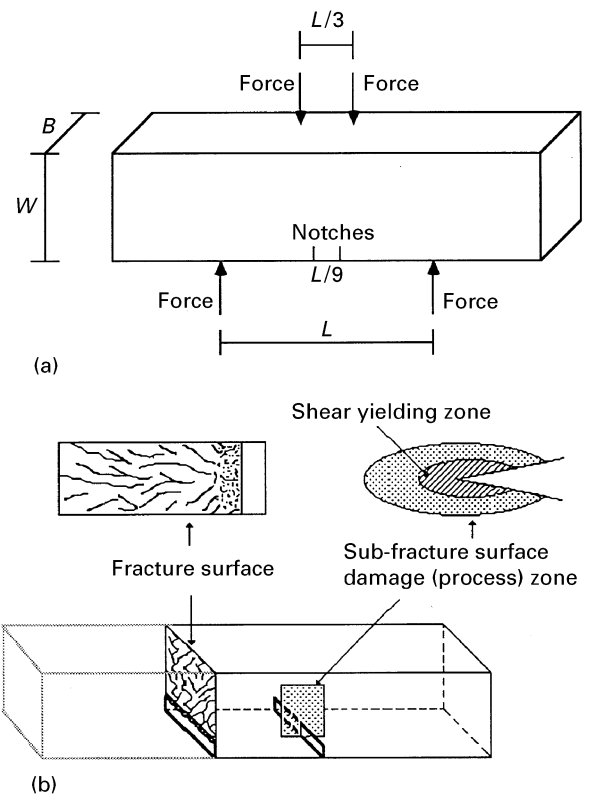


Figure 1 Schematics of (a) the DN-4PB geometry and (b) the regions utilized for TOM and TEM investigations.

zone (Fig. 1) were obtained by cutting and polishing, following the procedures described by Holik *et al.* [14]. The thin sections were made normal to the fracture surface but parallel to the cracking direction. These thin sections were then examined using an Olympus Vanox-S optical microscope both under bright field and crossed-polars.

In preparing the transmission electron microscopy (TEM) samples, the damage zone around the survived DN-4PB crack was cut along the thickness direction into two halves using a diamond saw. The damage zone in the plane strain core region of the specimen was carefully trimmed to an appropriate size, i.e., an area of  $\approx 5 \times 5$  mm, and embedded in DER\* 331 epoxy resin/diethylene triamine (12:1 ratio by wt). It was cured at 38 °C for 16 h. The cured block was then further trimmed to a size of  $\approx 0.3 \times 0.3$  mm with the crack tip in the damage zone roughly at the centre of the trimmed surface. Ultra-thin sections, ranging from 60 to 80 nm, were cut using a Reichert–Jung Ultracut-E microtome with a diamond knife. Should phase contrast need to be improved the thin sections would be placed in a vial containing 0.5% by weight of RuO<sub>4</sub> aqueous solution and stained for 20 min. The thin sections were then placed on 200-mesh formvar-coated copper grids and examined using a Jeol 2000FX ATEM operated at an accelerating voltage of 100 kV for TEM investigations.

### 3. Results and discussion

In an effort to study how the LC domain size varies with the curing conditions and to understand how the changes of LC domain size affect both fracture toughness and failure mechanisms of LCEs, the SEN-3PB and the DN-4PB experiments on LCE-1, LCE-2, and LCE-3 were conducted.

In measuring the fracture toughness of the LCEs, the SEN-3PB technique is employed. The results are shown in Table I. The fracture toughness values ( $G_{IC}$ ) among these three systems are found to be quite different. This implies that the morphology and fracture mechanisms in these systems are quite different, which are probably affected by how the LCEs are cured.

Table I also shows how the tensile modulus ( $E_t$ ) of the LCEs are affected by curing. When the LCE is allowed to cure slowly, i.e. the LCE-1 case, the  $E_t$  (4.2 GPa) becomes significantly higher than that of a typical conventional epoxy ( $E_t = 3.0$  GPa). However, if the LCE is cured rapidly, i.e. if there is still a significant portion of amorphous phase present (LCE-2 and LCE-3) [15], the  $E_t$  values will then be similar to conventional epoxies.

Indeed, when TOM investigation is conducted, the size of LC domain in the LCEs is found to vary significantly with how the LCE is cured (Figs 2–5). That is, when sufficient time is given for the relatively mobile mesogenic segments to align among themselves in LCE during cure, LC domains can grow to as big as 80  $\mu$ m in size (Figs 2 and 3). However, if

TABLE I Summary of the fracture toughness values in DGE-DHAMS/sulphanilamide systems

DGE-DHAMS/ sulphanilamide	$E$ (MPa)	$K_{IC}$ (MPa m <sup>1/2</sup> )	$G_{IC}$ (J m <sup>-2</sup> )	$T_g^a$ (°C)
LCE-1	4200	1.35 ± 0.06	380	215
LCE-2	2900	1.43 ± 0.08	580	235
LCE-3	3100	1.12 ± 0.06	350	225

<sup>a</sup> Obtained from the primary tan  $\delta$  peak of the dynamic mechanical spectrum [1].

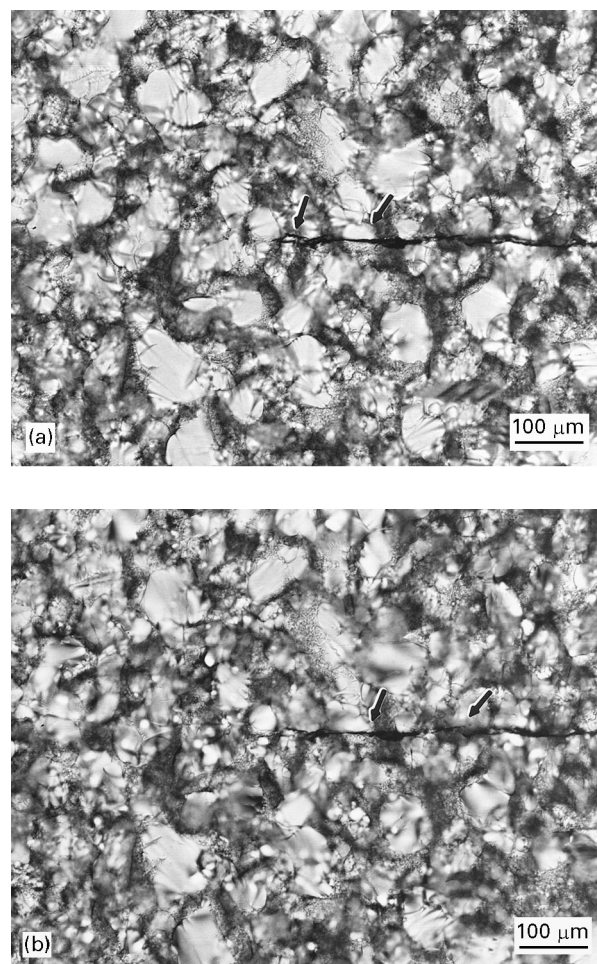
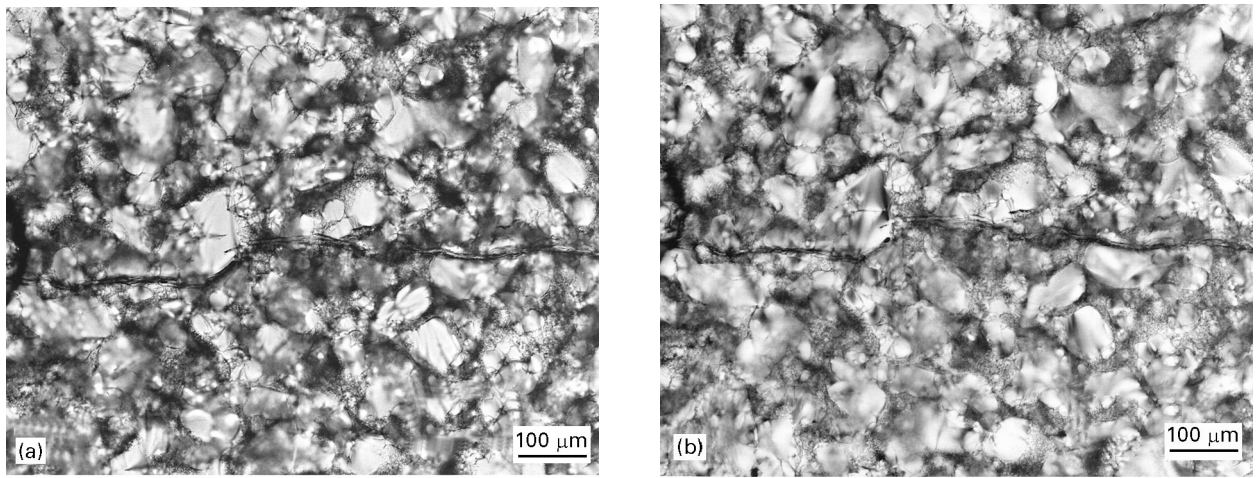


Figure 2 Transmitted optical micrographs taken at the DN-4PB crack tip damage zone of LCE-1 under (a) bright field and (b) crossed-polars. Large LC domains ( $\approx 80 \mu$ m in size) are found in this system. The crack appears to be able to penetrate the LC domains (see arrows).

the time allowed for forming the LC domains is reduced, the size of the LC domains in LCE becomes much smaller, i.e.  $\approx 3 \mu$ m (Fig. 4). Various shapes of LC domains were observed in this case. Some LC domains exhibit a cigar shape; while some LC domains appear to be spherulitical. This aspect will be further discussed in the TEM investigation below. When the LCE is cured at high temperatures, the rate of polymerization becomes so rapid that no time is

\* Trademark of The Dow Chemical Company.



*Figure 3* Transmitted optical micrographs taken at the wake of DN-4PB damage zone of LCE-1 under (a) bright field and (b) crossed-polars. The crack appears to propagate along the interstitial region of the LC domains.

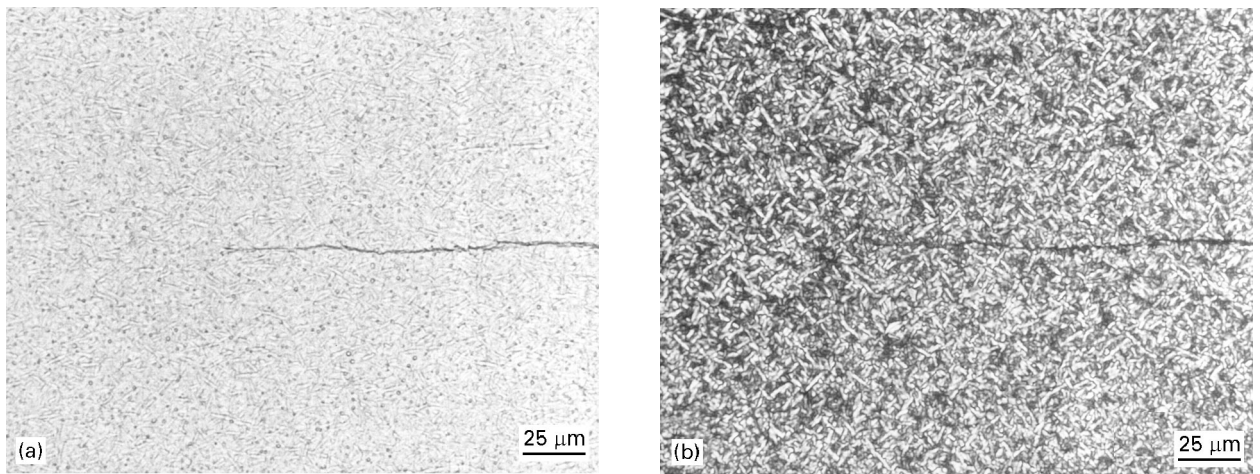


*Figure 4* Transmitted optical micrographs taken at the DN-4PB crack tip damage zone of LCE-2 under (a) bright field and (b) crossed-polars. The birefringent LC domains are rod-like in shape.

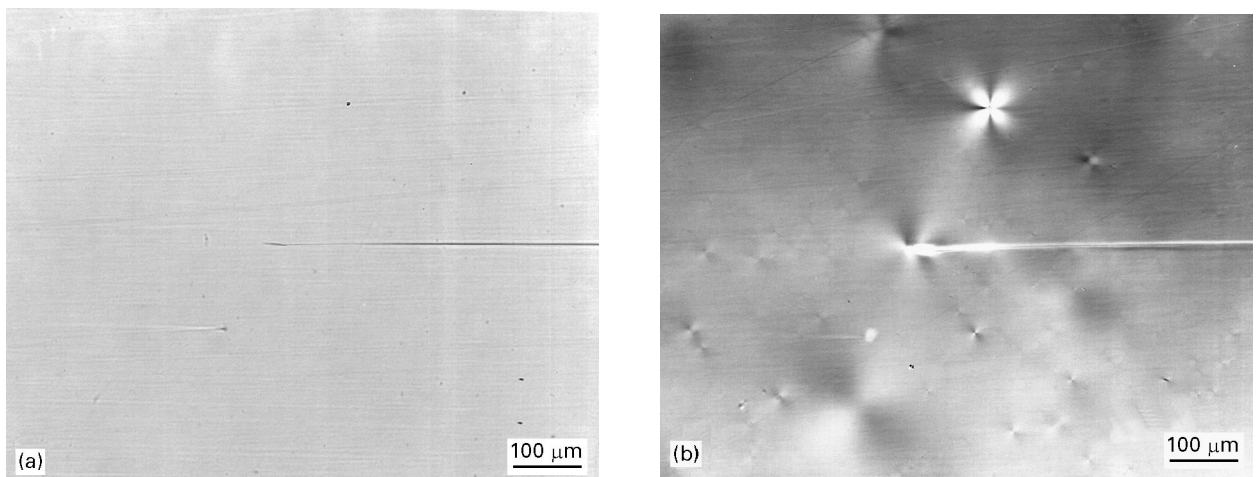


*Figure 5* Transmitted optical micrographs taken at the DN-4PB crack tip damage zone of LCE-3 under (a) bright field and (b) crossed-polars. No sign of domains is observed. The crack path is straight. Only limited crack tip plastic yielding is observed.

allowed for the mesogenic segments to form LC domains during the curing process [16]. As a result, no sign of LC domains is found in LCE-3 (Fig. 5). It is noted that the earlier small angle X-ray observations have indicated that the LC domains formed in LCE-1 and LCE-2 are smectic in nature [15–17]. The

dynamic mechanical spectroscopy and differential scanning calorimetry studies also suggested that these smectic domains, once formed, are thermally stable up to about 300 °C [8, 18].

The changes of the LC domain size in the LCEs appear to significantly affect the fracture process in the

LCE matrix. The TOM micrographs shown in Figs 2 and 3 clearly indicate that for the LCE-1 system, the crack preferably grows around the large LC domains, i.e. it is more difficult for the crack to grow through the well-developed LC domains in LCE-1. Therefore, the crack deflection mechanism dominates the fracture process. As for LCE-3, no sign of LC domains is found in the LCE matrix (Fig. 5). This leads to the growth of a straight, unperturbed, crack in the matrix.

In the case of LCE-2 system, as shown in Fig. 4, the LC domains appear to be in cigar shape and are much smaller in size ( $\approx 3\ \mu\text{m}$ ). Owing to the small size of the LC domains in the LCE-2, it is impossible to determine the fracture mechanisms operating in the LCE-2 system with TOM. TEM investigation of the damage zone in the DN-4PB specimen was carried out.

TEM investigation of the LCE-2 system shows direct evidence of the formation of various shapes of LC domains in the matrix (Fig. 6). The spherulitical/elliptical-shaped LC domains observed in LCE-2 may be due to the projection from the thick cigar shape LC domain on the plane of the thin section. Further

investigation is needed to ascertain the possible formation of other shapes of LC domains in this LCE system. When the crack propagates into this rather complex morphology, the crack appears to grow preferentially in the amorphous (or less organized LC) region and occasionally grows into the LC domains. This leads to the formation of a segmented crack in front of the main crack (see arrows in Fig. 7). Subsequently, when the crack opens up, the unbroken portion of the matrix acts as a bridge between the two opening crack planes (Fig. 8). Furthermore, since the segmented cracks are not formed on the same plane, when the crack propagates and eventually links with the segmented cracks, the crack branching mechanism becomes operative (Fig. 9). A higher fracture toughness value for LCE-2 is thus obtained.

The effect of curing condition on the formation of LC domains in LCEs is analogous to the cooling rate effect on the spherulite formation of semicrystalline thermoplastics, such as polypropylene [19]. The LC domain formation during curing has been found to be via the nucleation-growth mechanism [8]. When longer times are allowed for LCEs to cure, larger and

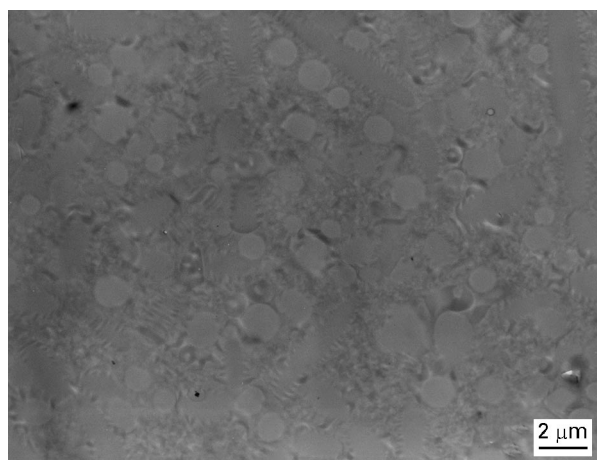


Figure 6 TEM micrograph showing the morphology of LCE-2. Various shapes of LC domains can be found in LCE-2.



Figure 8 TEM micrograph taken at the DN-4PB damage behind the crack tip of LCE-2. When the main crack opens up, the matrix material between the segmented crack acts as a bridge (see arrows) to resist crack propagation.

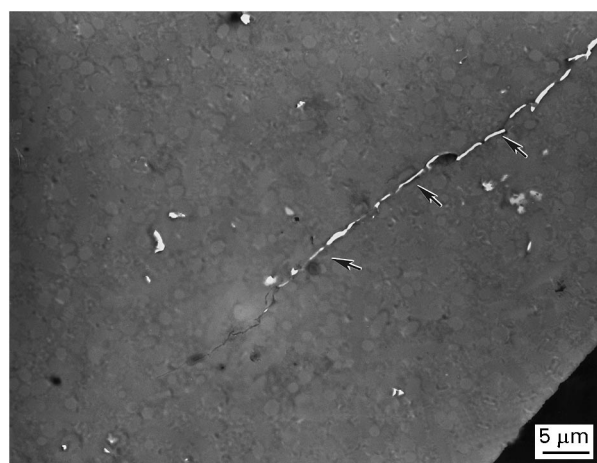


Figure 7 TEM micrograph taken at the DN-4PB crack tip damage zone of LCE-2. Formation of segmented cracks (see arrows) in front of the main crack is evident.

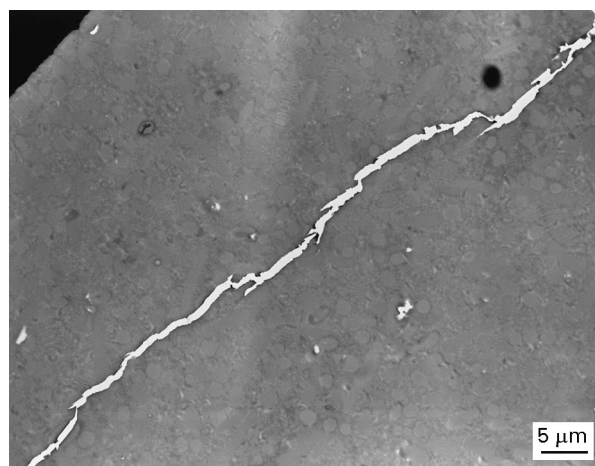


Figure 9 TEM micrograph taken at a crack wake region further behind that taken in Fig. 8. Repeated crack bifurcation are observed.

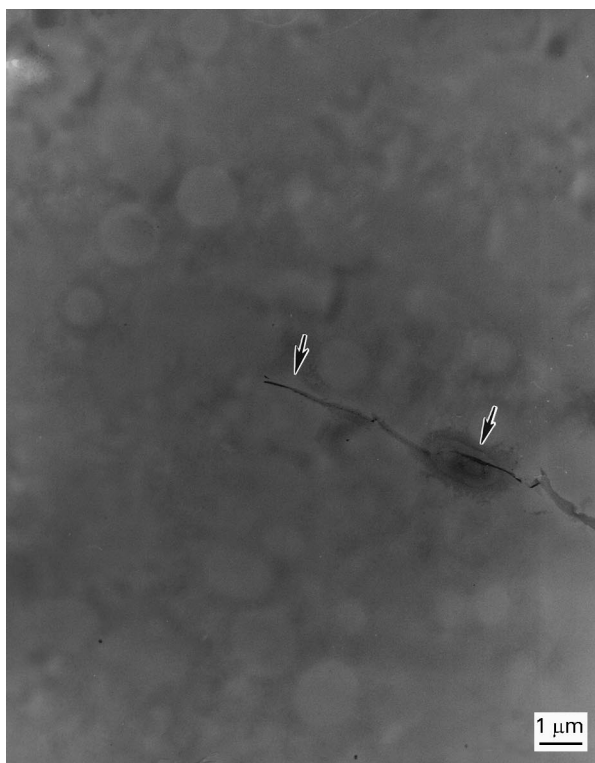


Figure 10 TEM micrograph taken at the DN-4PB crack tip damage zone of LCE-2. The crack grows through the LC domain (see arrows).

more perfect LC domains may form. When the LC domain is big and more perfect, the LCE material around the inter-LC domain region will usually contain either defects or low molecular weight species. This allows the crack to propagate, with little resistance, along the inter-LC domain region (Fig. 3). However, in contrast to the conventional spherulites, the crack appears to be able to occasionally grow across the LC domains (see arrows in Fig. 2). It is noted that the volume fraction of the ordered smectic phase in LCE-1 is estimated to be 39% [15].

On the other hand, if the time allowed for LCEs to cure is limited, the size of the smectic LC domains is smaller. Also, the structure inside the LC domains is likely to be less perfect. This makes the LC domains less resistant to crack penetration. Indeed, the crack is found to propagate through the LC domains more readily in LCE-2 (see arrows in Fig. 10), which probably has lower crystallinity than LCE-1. Many unique fracture mechanisms ensue in LCE-2 (Figs 6–10).

The apparent bridging mechanism observed in LCE-2 (Fig. 8) suggests that the LCE matrix is quite ductile in nature. In other words, when the triaxial stress state in front of the main crack is relieved by the formation of the segmented cracks, the matrix material between the opening crack planes is capable of significant plastic drawing. This will definitely help resist crack propagation in the LCE-2 matrix.

At this stage, even though the relationship between the LC domain size (which is affected by the curing conditions) and fracture behaviour is understood, we are still unable to clearly identify the local LC domain

structures. The lack of resolution of the selective-area electron diffraction and X-ray scattering [20] techniques in probing possible variations of molecular structure arrangement in the LC domain makes it impossible to verify any possible occurrence of transformation toughening and/or orientation toughening mechanisms, which would be unique for crystalline and liquid crystalline polymers, around the crack tip and the crack wake. The links between the local LC domain structural orientation and its perfection with the fracture behaviour of the LCEs are, therefore, unclear and are subject to future investigations.

#### 4. Conclusion

The fracture toughness and failure mechanisms of the DGE-DHAMS/sulphanilamide LCEs cured under various conditions were investigated using the SEN-3PB, DN-4PB, TOM and TEM techniques. The morphology in LCEs is found to be strongly dependent on curing schedule. Crack deflection, crack bifurcation, segmented cracking and crack bridging are found to operate in LCE-2, while for LCE-1, crack deflection is the major source of toughening. In the case of LCE-3, where no observable LC domains are found, the crack path is straight. Only limited crack tip yielding is observed.

#### Acknowledgements

The authors would like to thank E. I. Garcia-Meitin, W.-L. Huang, N. A. Orchard, M. I. Villarreal, M. D. Heaney, M. Cheatham, J. L. Bertram, and W. R. Howell, for their experimental assistance and discussion with this work.

#### References

1. J. D. EARLS and R. E. HEFNER, JR and P. M. PUCKETT, US Patent 5,463,091, 1995.
2. R. A. WEISS and C. K. OBER, *ACS Symp. Ser.* **435** (ACS, Washington, DC, 1990).
3. A. A. COLLYER, "Liquid crystal polymers: from structures to applications" (Elsevier Applied Science Publishers, New York, 1992).
4. G. C. BARCLAY, C. K. OBER, K. I. PAPATHOMAS and D. W. WANG, *J. Polym. Sci. Part A: Polym. Chem.* **30** (1992) 1831.
5. A. A. ROBINSON, S. G. McNAMEE, Y. S. FREIDZON and C. K. OBER, *Polymer Preprint* **34** (1993) 743.
6. J. D. EARLS and R. E. HEFNER, JR. and P. M. PUCKETT, US Patent 5,218,062, 1993.
7. M. E. SMITH, B. C. BENICEWICZ, E. P. DOUGLAS, J. D. EARLS and R. D. PRIESTER, *Polymer Preprint* **37** (1996) 50.
8. Q. LIN, Ph.D. Thesis, The University of Michigan, Ann Arbor, 1994.
9. H. J. SUE, R. A. PEARSON, D. S. PARKER, J. HUANG and A. F. YEE, *Polymer Preprint* **29** (1988) 147.
10. H. J. SUE and A. F. YEE, *J. Mater. Sci.* **28** (1993) 2915.
11. H. J. SUE, *Polym. Eng. Sci.* **31** (1991) 270
12. O. L. TOWERS, "Stress intensity factor, compliance, and elastic  $\eta$  factors for six geometries" (The Welding Institute, Cambridge, UK, 1981).
13. ASTM standard, E399-81.

14. A. S. HOLIK, R. P. KAMBOUR, S. Y. HOBBS and D. G. FINK, *Microstruct. Sci.* **7** (1979) 357.
15. H. HRISTOV and A. F. YEE, private communication.
16. Q. LIN, A. F. YEE, J. D. EARLS, R. E. HEFNER, JR. and H.-J. SUE, *Polym. Comm.* **35** (1994) 2679.
17. R. A. BUBECK, private communication.
18. Q. LIN, A. F. YEE, H. J. SUE, J. D. EARLS and R. E. HEFNER JR., *J. Polym. Sci. Polym. Phys. Ed.*, Dec. 1996 (in press).
19. E. HORNBOGEN and K. FRIDRICH, *J. Mater. Sci.* **15** (1980) 2175.
20. M. D. HEANEY, H. J. SUE, J. D. EARLS and R. E. HEFNER, JR., in preparation.

*Received 11 July  
and accepted 23 October 1996*